

# Next Generation Millimeter-wave Radar for Safe Planetary Landing

Brian D. Pollard and Gregory Sadowy  
Jet Propulsion Laboratory  
California Institute of Technology  
4800 Oak Grove Drive  
Pasadena, CA 91109  
818.354.7718  
pollard@jpl.nasa.gov

*Abstract*— Safe, precise landing on planetary bodies requires knowledge of altitude and velocity, and may require active detection and avoidance of hazardous terrain. Radar offers a superior solution to both problems due to its ability to operate at any time of day, through dust and engine plumes, and ability to detect velocity coherently.

While previous efforts have focused on providing near term solutions to the safe landing problem, we are designing radar velocimeters and radar imagers for missions beyond the next decade. In this paper we identify the fundamental issues within each approach, at arrive at strawman sensor designs at a center frequency at or around 160 GHz (G-band). We find that a G-band radar velocimeter design is capable of sub-10 cm/s accuracy, and a G-band imager is capable of sub-0.5 degree resolution over a 28 degree field of view. From those designs, we arrive at the key technology requirements for the development of power and low noise amplifiers, signal distribution methods, and antenna arrays that enable the construction of these next generation sensors.

## TABLE OF CONTENTS

1. INTRODUCTION.....	1
2. TERMINAL DESCENT SCENARIO.....	2
3. VELOCIMETRY.....	3
4. HAZARD DETECTION.....	4
5. HARDWARE DEVELOPMENT PLAN.....	6
6. SUMMARY .....	6
ACKNOWLEDGEMENT .....	6
REFERENCES .....	6

## 1. INTRODUCTION

Past Mars landing missions have been accomplished through the use of robust landing systems, including the use of landing gear on the Viking landers, or airbags on the Pathfinder and twin Exploration rovers. Future missions, however, are likely to employ less robust landing systems, as they allow the delivery of more massive scientific payloads for long term roving and sample returns. Those missions include the 2009 Mars Science Laboratory (MSL), described more fully in the next section.

<sup>1</sup>0-7803-7651-X/03/\$17.00/© 2004 IEEE

<sup>1</sup> IEEEAC paper #1188, Submitted Oct 20, 2004

Less robust landing systems place more stringent requirements on touchdown velocity and site selection, calling for improved capabilities in the sensing of navigation data, including altitude and three dimensional velocity, and in hazard detection. A previous paper [1] describes one approach based on an imaging radar at either W- or Ka-band. This sensor is designed to meet the requirements of MSL, including 10 cm/s accuracy on each velocity component, and 10 cm/pixel topographic maps for hazard detection, with approximately 1000 pixels over a 28° x 28° field of view.

Much of our work following the publication of [1] focused on developing a Ka-band sensor; this choice of frequency was necessitated by the delivery schedule of a 2009 opportunity, given the technology maturity of components. The disadvantages of Ka-band are of course the larger antenna size and mass associated with the resolution requirements.

More recently, we have begun to focus on developing radar velocimetry and imaging techniques for missions beyond 2009. In order to reduce antenna size and mass, we are designing sensors with a center frequency at G-band (160 GHz). This approach is now feasible due to the recent and upcoming availability of power amplifiers and low noise amplifiers, facilitating the design of a radar transmitter and receiver [2].

In this paper, we describe current G-band sensor design concepts, including both a radar velocimeter with the potential for extremely high velocity precision (1% of total, to 1 cm/s), and an imaging radar with 0.5 degree resolution per pixel. We discuss key system challenges with each concept, including problems of terrain slope and velocity ambiguities with high frequency velocimetry, and the potential for frequency scanning while maintaining a high system bandwidth for hazard detection imaging. Finally, we discuss our hardware development plan, which is nominally focused on developing the building blocks for these next generation sensors.

## 2. TERMINAL DESCENT SCENARIO

As the defining mission for a new class of landers, MSL continues to serve as the baseline for terminal descent remote sensing requirements development. While an early

version of the basic terminal descent scenario is discussed fully in [3] (and the references therein), the MSL project has more recently moved to the “sky crane” concept. In this section, we briefly describe this scenario, which is illustrated in Figure 1.

The entry phase consists of initial entry into the Martian atmosphere, and, once the vehicle has slowed and reached an altitude of nominally 8 km above the surface, the deployment of a supersonic parachute. Throughout this phase, the entire lander is encased in a heat shield and backshell, protecting against aerodynamic loads and heating, and prohibiting any terrain sensing.

After the vehicle has slowed to an appropriate velocity (at and altitude of some 3-5 km), the backshell and supersonic parachute are jettisoned, a subsonic parachute is deployed, and the heatshield is jettisoned. At this point, the radar can commence operation.

The lander remains on the subsonic parachute until an altitude of 500 to 600 m, at which time the chute is jettisoned and descent engines are ignited. If hazard detection capability is available, the vehicle is then turned toward the minimum fuel contour point, hazard detection scans are taken by the radar, and a safe landing site is chosen. At this point, there are approximately 30 seconds left until touchdown. The amount of propellant available

can allow for a maximum 100 m horizontal divert from the 500 m altitude.

Under the power of the descent engines, the lander maneuvers to a point nominally 5 m above the chosen landing site. At this point, the horizontal velocity must be nulled. The descent stage and rover then separate, and the rover is lowered to the surface via a tether. Upon touchdown the tether spools of the end of the reel, and the descent stage flies away from the rover landing site, crashing into the Mars surface.

Based on the present design, the rover must touch down with a horizontal velocity of less than 0.5 m/s. Further, safe landing requires slopes to be less than 30°, and rocks must be smaller than 0.75 m on flat terrain, or 0.1 m on sloped terrain. These touchdown requirements drive both the velocimetry and hazard detection requirements discussed in the next section.

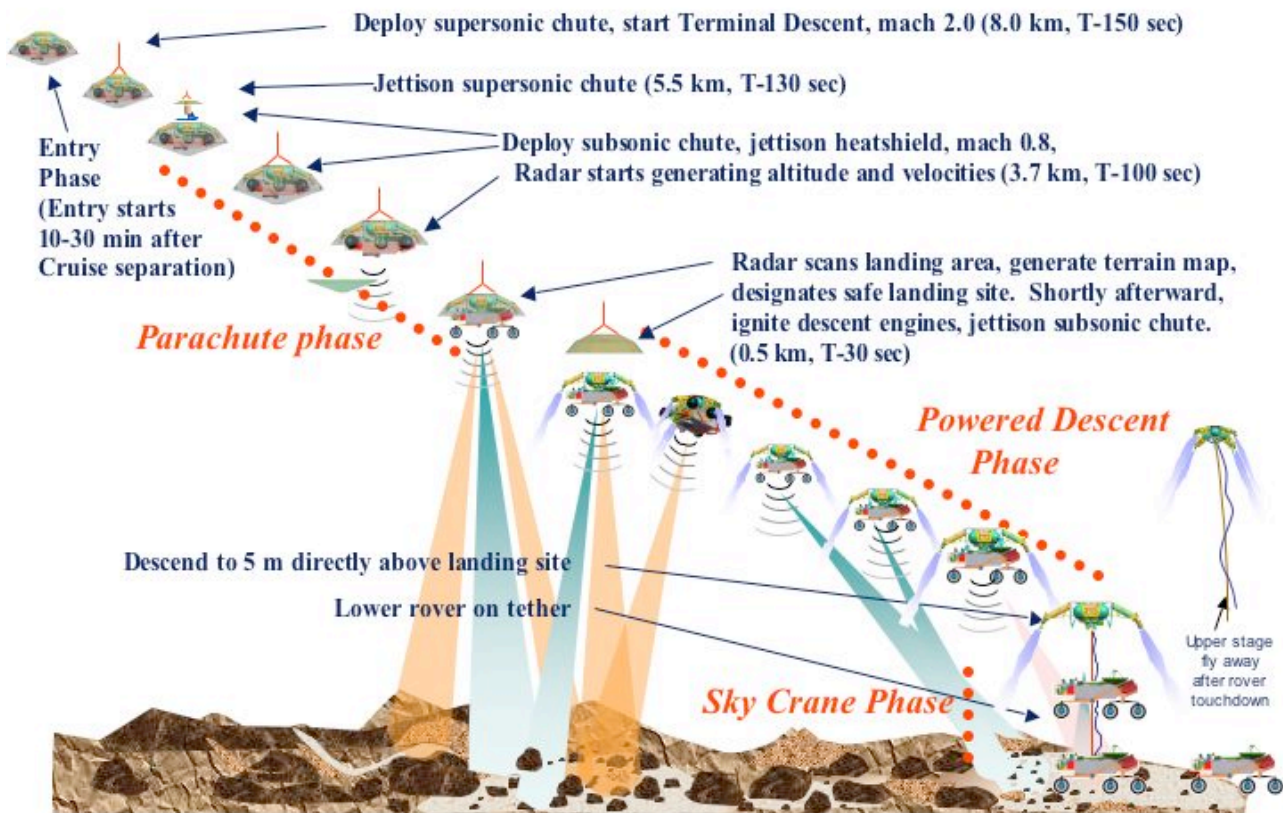


**Figure 1:** Sky crane terminal descent scenario similar to that in [3], but modified by E. Wong to fit the sky crane scenario.

### 3. VELOCIMETRY

As shown in the previous section, the sky crane has the capability to deliver delicate, massive payloads to the surface. A key requirements, however, is the ability to detect accurate velocities to better than 10 cm/s, the allocation given by MSL to the velocity sensor.

Past velocity sensors for terminal descent stages of planetary landers have included both radar (Viking and Polar Lander) and a camera / altimeter system (Exploration Rovers). The latter [4] produced 1 m/s [TBD] results but makes use of a passive camera, requiring daytime, dust free landing conditions. The passive camera approach is also incoherent, using the time separation of terrain features. Such an approach can, in theory, have trouble with terrain with too few features for tracking.

Radar can overcome the problems of a passive camera, allowing day/night operation, seeing through all but the most severe dust storms, and using coherent methods for velocity retrieval, correlating speckle from successive returns. In terms of implementation, however, the most recent example of a Doppler radar velocimeter for planetary landing, Mars Polar Lander (MPL), suffered from problems of radar beam / terrain interactions that are discussed in the following subsection.

#### *The Problem of Slope for a Wide Beam Sensor*

Due to cost and accommodation constraints, the Mars Polar Lander radar altimeter / velocimeter abandoned the narrow, pencil beam velocimetry approach used on Viking for one based around a wide beam, modified Pathfinder altimeter. The MPL sensor has four beams: one nadir pointing altimeter beam, and three canted velocimeter beams. The radial velocity is measured in each of the three beams via a Fourier transform in order to derive the three dimensional velocity vector.

Because each beam has a broad beamwidth, the velocity processor on the MPL radar uses the altitude and simple trigonometry to solve for the appropriate range gate in which to sample the radial velocity. Figure 2 illustrates the problem. Based on a measured altitude  $h$  and a boresight angle of  $\phi$ , the appropriate range gate  $\rho$  is selected as  $h/\cos(\phi)$ .

As seen in Fig. 2, however, this approach produces an error when the terrain has a significant slope. In particular, the angle of arrival of the signal,  $\phi'$ , is not as expected given a ground slope  $\theta$ . One can derive the angle difference between  $\phi$  and  $\phi'$  as

$$\delta\phi = \cos^{-1}\left(\frac{\rho^2 \cos^2(\theta) + h^2 \cos^2(\theta) - \rho^2 \sin^2(\phi)}{2h\rho}\right) - \cos^{-1}\left(\frac{h}{\rho}\right) \quad (1)$$

Equation (1) converges to zero for  $\theta = 0$ , as expected.

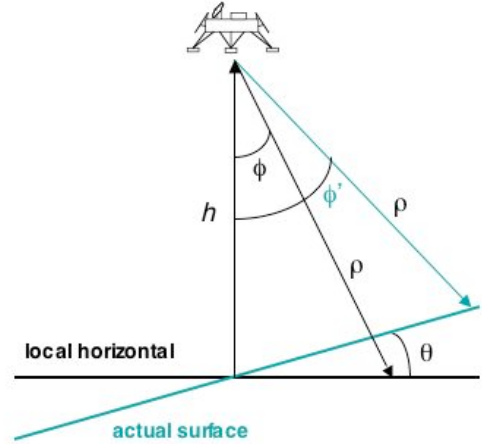


**Figure 2:** Radar velocimeter measurement geometry.

The angle error expressed in Eq. (1) produces a mixing of horizontal and vertical velocities, important for landers, where the vertical velocity component is typically much larger than the horizontal. Again, from simple geometry, the horizontal velocity error  $\delta v_h$  is

$$\delta v_h = \frac{v_h(\cos\phi' - \cos\phi) - v_v(\sin\phi' - \sin\phi)}{\cos(\phi)}. \quad (2)$$

The angle bias in Eq. (1) is large: at a look angle of  $20^\circ$ , the angle bias incurred from a  $30^\circ$  slope is  $25^\circ$ . From Eq. (2), some 40% of the vertical velocity mixes into the horizontal component; for a 10 m/s vertical velocity, the horizontal velocity error would be at least 4 m/s, even if the actual horizontal velocity were zero. Given the high vertical velocities during the descent stage, this produces unacceptably large errors.

The solution to the problem of slope is to of course bound the angle of arrival problem, either through measurement of the angle (such as a phase monopulse system), or through a very narrow beam sensor. One very distinct advantage of a G-band radar velocimeter is that a very narrow beamwidth can be made from a physically small antenna.

#### *G-band Velocimeter Performance*

To reach sub-1cm/s biases during a sky crane phase, one must reduce the angle bias in Eq. (2) to less than  $0.5^\circ$ , or a  $1^\circ$  full cone beamwidth. The advantage of G-band for such a narrow pencil beam becomes clear: a  $1.0^\circ$  beamwidth requires only a 13 cm antenna.

By eliminating terrain biases in the velocimeter measurements, we are free to concentrate on systematic and random error sources within the sensor itself. Those depend entirely on the method by which the velocity is estimated.

We use the “pulse-pair” technique [5] (also described in [1]) to estimate the first moment of the received Doppler spectrum; FM-CW is ruled out due to the need for multiple beams under a single controller. Given a pulse transmitted at time  $t_1$ , with a range to the surface along the boresight vector of  $\rho_1$ , and a second pulse transmitted at  $t_2 (= t_1 + \Delta t)$ , with a range of  $\rho_2$ , the argument of the correlation product,  $q$  of the two returns ( $s_1$  and  $s_2$ ) is

$$q = \arg(s_1 s_2^*) \quad (3)$$

where  $s_1$  and  $s_2$  are the received signals at  $t_1$  and  $t_2$  respectively. The mean velocity is then

$$v = \frac{-q\lambda}{4\pi\Delta t} \quad (4)$$

The error in estimating the line of sight velocity can be calculated as [6]

$$\sigma_v = \frac{\lambda}{2} \frac{\sqrt{\gamma^{-2}(\Delta t)(1 + SNR^{-1}) - 1}}{\sqrt{2N}2\pi\Delta t} \quad (5)$$

where  $N$  is the number of looks,  $SNR$  is the signal-to-noise ratio, and  $\gamma(\Delta t)$  is the target correlation coefficient.

Achieving 1% velocity standard deviation as expressed by Eq. (5) can be achieved for pulse pair intervals less than the ambiguous velocity interval,  $\Delta t = \lambda / v$ . In fact, if we set  $\Delta t = \lambda / 2v$ , we can arrive at an expression

$$N \cdot SNR = \frac{1}{p^2 8\pi^2} \quad (6)$$

where  $p$  is the desired velocity standard deviation ( $\sigma_v/v$ ), and the correlation term has been neglected. For  $p=0.01$ , the looks-SNR product must be larger than 126.6; in other words, for 10 looks, we require 11 dB SNR, both quite reasonable.

Such an approach merely requires that the optimum pulse pair interval be always used (within a factor of two). This type of timing must be adaptive, due to the rapidly changing velocities during descent, and has already been designed into the Ka-band sensor for MSL, based on work originally done for atmospheric radar timing [7]. No unwrapping of ambiguous velocities is required.

Regarding systematic errors, we note that phase biases over the pulse pair interval time (shorter than 1 ms) will be extremely small. Thus the systematic errors due to antenna movement or insertion phase differences within the system should be small, and the noise should be dominated by the thermal component expressed in Eq. (5).

#### Velocimeter Design Considerations

As expressed in the previous section, a target SNR for a velocimeter is 11 dB over an entire range of operation. Table 1, below, shows a sample set of radar parameters, while Table 2 shows the associated radar range equation

values. Key to note are the peak transmit power of the system, set to 0.1 W, the antenna size, set to 20 cm x 20 cm, and the noise figure of 8 dB. Those values will be discussed more fully in the development plans that follow.

**Table 1:** Strawman G-band velocimeter parameters.

Parameter	Unit	Value
Center Frequency	GHz	160
Wavelength	mm	1.9
Peak Transmit Power	W	0.1
Front-end One Way Loss	dB	3.0
Antenna Dimensions	cm x cm	20.0 x 20.0
Antenna Efficiency	%	50
Sigma0	dB	-10
Bandwidth	MHz	10-400
Pulsewidth	ns	60-2000
Pulse Repetition Freq.	kHz	~100
Receiver Noise Figure	dB	8.0

**Table 2:** Radar range equation tables (in dBW) for ranges of 100 m and 3500 m. At 100 m, a pulsewidth of 60 ns and bandwidth of 400 MHz is assumed. At 3500 m, a pulsewidth of 2  $\mu$ s and a bandwidth of 10 MHz is assumed.

Parameter	Value [dBW] R=100m	Value [dBW] R=3500m
Peak Transmit Power	-10.0	-10.0
Two-way Losses	-6.0	-6.0
Two-way Antenna Gain	103.1	103.1
Two-way Antenna Efficiency	-6.0	-6.0
Sigma0	-10.0	-10.0
Ground Area	0.1	31.2
Range Loss	-80.0	-141.8
$\lambda^2/(4\pi)^3$	-87.5	-87.5
Range Compression Gain	13.8	13.4
Signal Power	-82.5	-113.6
Noise Power	-110.0	-125.6
<b>Signal to Noise Ratio</b>	<b>27.4</b>	<b>12.0</b>

Critical to maintaining constant SNR over the large altitude range of the landing system is the ability to change adaptively the bandwidth / pulsewidth combination as a function of range. With a maximum pulsewidth of ~2  $\mu$ s (given the pulse pair interval required at high altitude of ~10  $\mu$ s), the lower bandwidth range is set accordingly to 10 MHz. The upper bandwidth range of 400 MHz is more than sufficient for all key altimetry applications (not discussed here, but a consideration for all terminal descent sensors).

In summary, two of the key aspects of a high frequency velocimeter design are in digital control: the adaptive ability to change pulse pair interval, bandwidth, pulse width, and of course pulse repetition frequency as a function of range. Further work in this program will look at extending the Ka-band timing unit design to accommodate this type of agile radar control and timing.

In addition to the digital control, we also note that reasonably aggressive values have been assumed for peak transmit power, noise figure, and antenna size and performance. Those aspects are discussed in our hardware development plan in Section 5, below.

#### 4. HAZARD DETECTION CAPABILITY

The sky crane concept introduced in Section 2 has the ability to tolerate modest hazards, such as 0.75 m rocks on flat terrain, or slopes as large as 30°. On Mars, however, landing in terrain near large craters, more probable to have rocks over 0.75 m [8], or in terrain with steep slopes, including canyon walls, may require active detection and avoidance.

MSL adopted the Ka-band sensor described in [1] due to its day/night operational capability, ability to see through or near engine plumes, and the quality of its navigational data. The sensor configured for MSL has a stated requirement of detecting craters in the range of 50-200 m in diameter from an altitude of 500 m. Those requirements are met through the use of a 65 cm antenna (~0.9° beamwidth) and a field of view of 28° x 28°.

The choice of a minimum crater size of 50 m is somewhat arbitrary from a landing site perspective, and is driven instead by accommodation of the large antenna. As for velocimetry, the desire for future missions is to maximize the available resolution from a reasonably sized antenna. Within this section we explore both the hazard detection requirements as well as potential radar implementation options for next generation missions.

##### *Hazard Detection Requirements*

Analysis performed for MSL (A. Johnson, personal communication) clearly states that a sensor with approximately twice the resolution capabilities of that planned for MSL would have a significant impact of the probability of a safe landing, reducing the probabilities to better than nearly 99% even in heavily cratered terrain. This capability translates into the key requirements summarized in Table 3. They include the ability to scan an area of 28° x 28° every 1 second with a beam resolution of less than 0.5°.

**Table 3:** Summary of key hazard detection requirements.

Requirement	Value
Sensor Field of View	28° full cone
Image Beamwidth	0.5° / pixel
Image Frame Rate	1 Hz

As for velocimetry, we desire to achieve the beam resolution with an aperture that is as small and light as possible, and again, given the state of technology development, we choose to examine the capabilities at 160 GHz. At that center frequency, the aperture size would be ~27 cm in diameter. The element dimensions to meet the 28° field of

view requirements would need to be ~4.5 mm. This combination would require, for a nominal filled aperture, approximately 4000 individual elements. While the Ka-band sensor in [1] used a thinned array to reduce the number of elements, and thus cost and mass, the large amount of available bandwidth at higher frequencies enables steering techniques like frequency scanning to be employed.

##### *Frequency Scanning and Antenna Sizing*

Frequency scanned antennas offer a simple solution to the problem of scanning in one of the two dimensions without the use of phase shifters or time delay modules. These antennas have a long history in air-search radar (such as the SPS-48 and its predecessors), and are relatively simple to manufacture, at least at lower frequencies. While at lower frequencies one usually must sacrifice bandwidth (resolution) for scanning capability, at 160 GHz, the available percentage bandwidth is such that reasonable resolution may be maintained while keeping a reasonable number of scan locations. For example, a 28° field of view and 0.45° beamwidth require some 64 beam positions. Assuming a 500 MHz total bandwidth is required per beam for appropriate range resolution, the resultant total system bandwidth is 32 GHz. While large by most standards, this represents 20% total system bandwidth, which is achievable.

With a frequency scanned (or other 1D surface scanning method) enabling one dimension of scanning, the number of modules and phase shifters can be reduced to approximately 64, given our 27 cm antenna and 4.3 mm element size. This number of transmit/receive modules and phase shifters is much more realizable than even a thinned version of a 2-D electrically scanned array.

##### *Strawman System Design & Capabilities*

Based on the frequency scanned design described above, we can summarize the key characteristics of a 160 GHz hazard detection sensor as follows in Table 4.

**Table 4:** Key parameters of a hazard detection design.

Parameter	Value
Center Frequency	160 GHz
Total System Bandwidth	32 GHz
Bandwidth per Beam	400 MHz
System Noise Bandwidth	500 MHz
Number of Active Elements	64
Sensor Field of View	28° full cone
Sensor Beamwidth	0.5° / pixel
Power per Element	10 dBm
Noise Figure per Element	8 dB
SNR at 3500 m	10 dB

Such a sensor would fit within a relatively small footprint, have a mass below that of the Ka-band antenna designed for MSL (9 kg), and use much of the control and timing logic designed for MSL.

## 5. HARDWARE DEVELOPMENT NEEDS & PLANS

The strawman designs in the previous sections are put forward to motivate our near term research: development of key technology building blocks toward an eventual 160 GHz sensor. As seen above, the key technology elements include:

- Frequency scanning (or other tunable aperture), wide bandwidth antennas,
- Pulsed power amplifiers with output powers at and above 10 dBm,
- Low noise amplifiers with noise figures at or below 8 dB, and
- Phase shifting methods.

In addition, if we wish to avoid the need for separate transmit and receive antennas, a waveguide circulator or other transmit/receive switch must also be developed.

Under this new program, we are preparing to address in particular the amplifier challenges by building on previous JPL programs [2]; we are in the process of developing power amplifier and receiver MMICs and associated packaging that are a first step toward implementation of a G-band receiver. In addition, current system studies are focusing on the key and secondary technology challenges associated with the antenna. Those include phase shifting and signal distribution for both velocimetry and hazard detection designs.

Ultimately, our goal is to integrate the above developments into a functional antenna, and marry such an antenna to the Ka-band control and timing hardware, completing a prototype sensor in time for infusion into a mission in the decade following MSL.

## 6. SUMMARY

Future missions requiring high precision velocimetry must overcome problems of terrain interactions while maintaining a reasonable sensor footprint on the landing vehicle; for that reason, we propose the development of G-band radar velocimeters that can achieve extremely high accuracy and precision (sub 10cm/s) from a reasonable antenna size. Future hazard detection requirements of sub-degree resolution with nearly 30° field of view require also point to phased arrays at similar frequencies.

The needs for future technology developments have been set through two strawman designs: a high accuracy velocimeter, and an imaging radar, both at 160 GHz. Both have the capability to meet the requirements of a large variety of less than robust landers in a reasonably sized package.

Our future work plans are threefold. First, we are specifically focused on the development of key sensor building blocks, including MMIC power and low noise amplifiers with sufficient bandwidth, power, noise figure, and manufacturing repeatability; second, we are addressing other system configuration issues, including problems of signal distribution, phase shifting, and non-phase scanning

antennas; and third, we are examining system algorithm and timing issues that can improve the performance of these sensors.

Finally, we hope to continue discussions with various mission designers and system engineers involved in future planetary landers. While the requirements here are based around the needs of MSL, the inputs from other users help significantly in the development of these unique sensors.

## ACKNOWLEDGEMENT

This work was performed at the Jet Propulsion Laboratory, California Institute of Technology, under contract with the National Aeronautics and Space Administration (NASA). The authors wish to acknowledge Edward Wong, Andrew Johnson, Dan Burkhart, and Tim Crain for their assistance in defining the requirements on the radar for the Mars Science Laboratory mission, and Sam Thurman for his rendition of Figure 2.

## REFERENCES

- [1] B.D. Pollard, G. Sadowy, D. Moller, and E. Rodríguez, "A millimeter-wave phased array radar for hazard detection and avoidance on planetary landers," *Proceedings of the 2003 IEEE Aerospace Conference*, Big Sky, MT, March 2003.
- [2] L. Samoska, A. Peralta, J. Bruston, "Advanced HEMT MMIC circuits for millimeter and submillimeter power sources", *Proceedings of the Far Infrared, mm and Sub-mm Detector Workshop*, Monterey, CA, April 2002.
- [3] E.C. Wong, G. Singh, J.P. Masciarelli, "Autonomous guidance and control design for hazard avoidance and safe landing on Mars (AIAA-2002-46192)," *Proceedings of the 2002 AIAA Atmospheric Flight Mechanics Conference*, Monterey, CA, August 2002.
- [4] Y. Cheng, J. Goguen, A. Johnson, C. Leger, L. Matthies, M.S. Martin, and R. Wilson, "The Mars exploration rovers descent image motion estimation system," *IEEE Intelligent Systems*, 19, 3, pp 13-21, 2004.
- [5] R.J. Doviak and D.S. Zmic, *Doppler Weather Radar Observations*, San Diego: Academic Press, 1993.
- [6] K.S. Miller and M.M. Rochwarger, "A covariance approach to spectral moment estimation," *IEEE Trans. on Information Theory*, vol. 18, no. 5, pp 588-596, 1972.
- [7] A.C. Berkun, M.A. Fischman, and E. Im, "An advanced on-board processor and adaptive scanning controller for the next generation precipitation radar," *Proceedings of the 2002 Earth Science Technology Conference*, 2002.
- [8] D.E. Bernard and M.P. Golombek, "Crater and rock hazard modeling for Mars landing (AIAA-2001-4697)," *Proceedings of the 2001 AIAA Space Conference*, Albuquerque, NM, August 2001.



**Brian D. Pollard** received the Ph.D. in Electrical and Computer Engineering from the University of Massachusetts at Amherst in 1998. His research at the Massachusetts



Laboratory included the development of a digitally beamformed volume-imaging radar for atmospheric boundary layer (ABL) studies, and compared data from that instrument to large-eddy simulations of the ABL. Dr. Pollard joined the Jet Propulsion Laboratory in 1998, where he has been active in the development of high accuracy radar interferometry, altimetry, and velocimetry sensors for planetary, oceanic, and terrestrial applications.

**Gregory Sadowy** received a B.S.E.E degree from the Rensselaer Polytechnic Institute in 1992 and a Ph.D. in E.E. from the University of Massachusetts at Amherst in 1999. He designed and managed development of the RF electronics for the NASA/JPL 95 GHz Airborne Cloud Radar and has



supported development of advanced RF electronics for the CloudSat Cloud Profiling Radar. He was responsible for the multi-frequency RF electronics for the Second Generation Precipitation Radar (PR-2) Airborne Demonstrator as well as a 35-GHz electronically scanned array for the PR-2 spaceborne precipitation radar. Dr Sadowy is currently developing a millimeter-wave phased array for hazard avoidance during Mars landings. His other research activities include advanced radar architectures and component development for large, flexible membrane phased-array radars.

